



Research report

Dynamic functional connectivity among neuronal population during modulation of extra-classical receptive field in primary visual cortex



Xiaoke Niu^a, Li Shi^{a,b,*}, Hong Wan^{a,**}, Zhizhong Wang^a, Zhigang Shang^a, Zhihui Li^a

^a School of Electrical Engineering, Zhengzhou University, Zhengzhou 450001, China

^b Department of Automation, Tsinghua University, Beijing 100000, China

ARTICLE INFO

Article history:

Received 1 December 2014

Received in revised form 3 July 2015

Accepted 8 July 2015

Available online 17 July 2015

Keywords:

Extra-classical receptive field

Surround modulation

Functional connectivity

Primary visual cortex

Granger causality

ABSTRACT

The neuronal activity evoked by stimuli confined in a receptive field can be modulated by surround stimuli of the extra-classical receptive field (eCRF). The surrounding modulation, hypothesized to be the basis of visual feature integration and figure-ground segregation, has drawn much attention in the field of neuroscience and engineering. However, most studies focused on surround modulation of individual neuronal response. In this study, we analyzed surround modulation of the population response recorded from rat primary visual cortex, and further investigated dynamic functional connectivity modulated by the surrounding stimuli. The functional connectivity was estimated using Granger causality (GC) and then determined by thresholding the p -matrix with different significance α values. Four scalar indexes were calculated to describe the functional connectivity of neuronal population: averaged connection strength (mGC), connection density (D), clustering coefficient (C) and path length (L). The statistical results from 5 rats showed that these network characteristics were dynamically changed during modulation of surrounding stimuli, which suggested that the neuronal population may connect in a dynamic way during modulation of eCRF. We further guessed that the neurons may happen to be organized in a more efficient way underlying surrounding modulation conditions, which helps to process larger images efficiently with the same number of neurons. This study provided new insights for a better understanding of the underlying neural mechanisms responsible for surround modulation.

© 2015 Elsevier Inc. All rights reserved.

1. Introduction

The stimuli surrounding the classical receptive field (CRF), cannot elicit spikes when stimulating alone, but can modulate the visual response to CRF stimuli (Barlow, 1953; Hubel and Wiesel, 1965; Cavanaugh et al., 2002a). This phenomenon refers to the so called “surround modulation,” which is hypothesized to be the basis of visual feature integration and figure-ground segregation (Albright and Stoner, 2002; Seriès et al., 2003). Furthermore, understanding the underlying neural mechanisms is important for developing a theoretical model of early signal integration and neural encoding of visual features in the primary visual cortex (V1).

Basic studies on surround modulation have shown that the surround stimuli modulated both the spiking activity of individual neurons and slow components (<250 Hz) of the extracellular potentials (local field potential, LFP) (Zhang and Li, 2013), the latter of which generally reflected synaptic inputs. Further studies have found that the surround modulation, mostly suppressive, was selective to visual features, such as orientation, spatial frequency, and stimulus size (Cavanaugh et al., 2002b; Webb et al., 2005), and that surround suppression for increasing stimulus size (“size tuning”) had preferred receptive field sizes that depended on contrast (Henry et al., 2013). It was also reported that the surround suppression would sharpen the orientation tuning (Okamoto et al., 2009) or enhance the orientation selectivity (Chen et al., 2005; Xing et al., 2005) of a single neuron in V1. Thus far, the majority of studies on surrounding modulation have concentrated on exploring the modulation of individual responses, such as the spiking activity at the single neuron level (Osaki et al., 2011; Henry et al., 2013) or LFP at individual recording locations (Gieselmann and Thiele, 2008; Zhang and Li, 2013), under the surrounding stimuli.

There were also many other attempts to explain the underlying neural mechanisms responsible for surround modulation and those

Abbreviations: RF, receptive field; CRF, classical receptive field; eCRF, extra-classical receptive field; GC, Granger causality; V1, primary visual cortex; LFP, local field potential.

* Corresponding author at: School of Electrical Engineering, Zhengzhou University, Zhengzhou 450001, China. Fax: +86 0371 67781407.

** Corresponding author. Fax: +86 0371 67781407.

E-mail addresses: shili@zzu.edu.cn (L. Shi), wanhong@zzu.edu.cn (H. Wan).

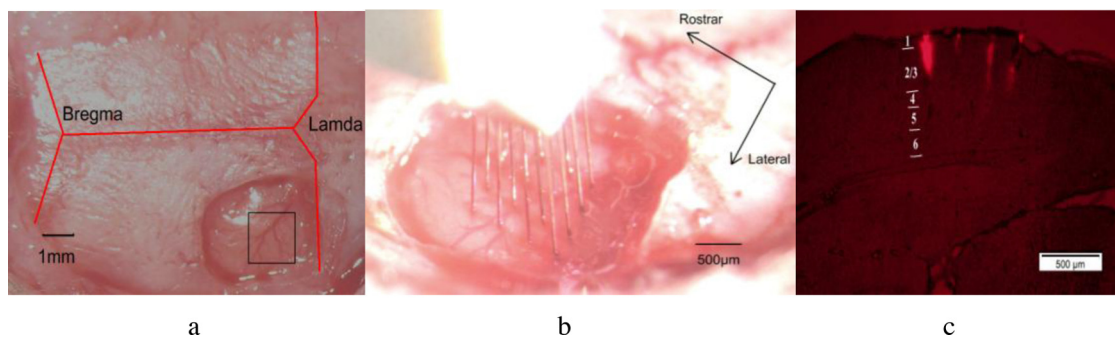


Fig. 1. Examples showing implantation of a 4×4 microwire electrode array in rat V1, and a histological slice used to verify electrode tracks in V1.

studies mostly hypothesized that the modulation of extra-classical receptive fields (eCRF) in V1 was a product of long-range horizontal connections (<5 mm) (DeAngelis et al., 1994; Dragoi and Sur, 2000; Stettler et al., 2002; Reynaud et al., 2012), and/or feedback from extrastriate areas (Angelucci et al., 2002; Sceniak et al., 2002; Bair et al., 2003; Wang et al., 2010; Nassi et al., 2013). There were also differing reports that response modulations by static texture surround in V1 were irrelevant to the feedback connections from V2 (Hupé et al., 2001) and might have resulted from local, short-range (<0.5 mm) lateral connections within V1 (Wieland and Sajda, 2005). The mechanisms remain unknown. Nevertheless, it could be speculated that the surround suppression phenomenon involved interactive activities of the neuronal population, and was associated with the interaction activities between individual neurons or between neuronal groups, locally and/or globally. In our study, we focused on investigating the surround modulation of functional connectivity among the neuronal population from V1, recorded with microelectrode arrays, without regard to the spatial scale. Considering the horizontal connections were frequently observed in layer 2/3 (Burkhalter, 1989; Stettler et al., 2002; Medini, 2011), and were much less affected by long-range axonal targets from higher areas (Brown and Hestrin, 2009), we mainly concentrated on analyzing the functional connectivity in layer 2/3 of V1.

With the rapid development of computational techniques for estimating the functional connectivity between or among neurons, powerful approaches have emerged (Yook et al., 2013). The commonly used statistical/computational methods were Granger causality (GC) (Achard et al., 2006; Guo et al., 2008; Ge et al., 2009; Ouyang et al., 2014), dynamic Bayesian inference (Lee et al., 2006; Neapolitan, 2009; Ide et al., 2014), the maximum likelihood model (Okatan et al., 2005), and the Ising model (Yu et al., 2008), of which GC analysis has become an increasingly popular method for identifying the causal connectivity in neural time series data (Barnett and Seth, 2011). Recently, it has also been used to reconstruct the underlying anatomical connectivity in conductance-based integrate-and-fire neuronal networks (Zhou et al., 2014).

In this study, we analyzed the modulation of averaged population responses, recorded from layer 2/3 of rat V1, against the size of the visual stimuli. The CRF and eCRF for the population were further approximated using the same method applied on individual neurons. The functional connectivity among the neuronal population was computed with the GC method (Barnett and Seth, 2014), under CRF alone and CRF combined with eCRF stimuli conditions. Four characteristics were measured to describe the dynamics of functional connectivity among neuronal population: connection strength (mGC), connection density (D), clustering coefficient (C) and path length (L). The statistical results proved that the surround stimuli would dramatically changed the functional connectivity among the neuronal population from V1.

2. Material and methods

2.1. Animal preparations

Our data were recorded from five Long Evans (LE) rats (2–4 months of age, 200–300 g) supported by the Animal Center of Zhengzhou University. All experimental procedures were in accordance with the guidelines of the National Institutes of Health and were approved by the Animal Care and Use Committee of Zhengzhou University.

Before surgery, each rat was anesthetized with urethane (1.3–1.5 g/kg body weight) and restrained in a stereotaxic apparatus (David Kopf Instruments, Tuhunga, CA, USA). The rectal temperature was monitored and body temperature was maintained at 37.5°C with a heating pad. The right eye was fixed with a metal ring to prevent eye movement, the pupils were dilated with topical application of 1% atropine sulfate, and the nictitating membranes were retracted with 5% phenylephrine. A craniotomy (diameter >2 mm) was performed over the left V1 with the core at 3 mm lateral and 7.5 mm posterior to the bregma (Fig. 1a). The microelectrode array (MEA) was implanted into the area (marked with a black square in Fig. 1a) after being dipped in 3% DiI solution (1,1'-dioctadecyl-3,3,3',3'-tetramethylindocarbocyanine perchlorate; invitrogen, Carlsbad, CA, USA) prepared with dimethylformamide (DMF) to label the track of the electrode insertions (Zhang and Zhang, 2010). The MEA consisted of 16 polyimide-insulated platinum/iridium microwires (Clunbury Scientific, Bloomfield Hills, MI, USA) that were arranged in four rows with four wires in each row (electrode diameter = $50\ \mu\text{m}$; electrode spacing = $350\ \mu\text{m}$; row spacing = $350\ \mu\text{m}$; impedance = $20\text{--}50\ \text{k}\Omega$). Then the array was lowered approximately 200–600 μm below the V1 surface (Fig. 1b), corresponding to layer 2/3 of V1, where horizontal connections could be frequently observed. Finally, a silver wire from the array was connected for grounding to bone screws inserted into the skull surrounding the surgical openings. The recording sites were finally examined with histological slices, under a fluorescence microscope (Fig. 1c, see Section. 2.7 for details).

2.2. Visual stimuli

Visual stimuli were generated from a PC running a Matlab toolbox (Psychtoolbox; MathWorks, Natick, MA, USA), and displayed on an LCD monitor (250×400 mm, refresh rate, 60 Hz) positioned 15 cm in front of the rat's right eye. The center of the receptive fields for individual neurons were determined with sparse noise stimuli, with a single bright square ($6.6 \times 6.6^\circ$) flashing on a black background at each of 12×12 positions in a pseudo random sequence (20 flashes/position). The spatiotemporal structure of RF was estimated with reverse correlation (Jones and Palmer, 1987). The spatial profile at each temporal delay was approximated with

Download English Version:

<https://daneshyari.com/en/article/4318683>

Download Persian Version:

<https://daneshyari.com/article/4318683>

[Daneshyari.com](https://daneshyari.com)